Title

Brief Report: Oxidative Stress Mediates Cardiomyocyte Apoptosis in a Human Model of Danon Disease and Heart Failure

Journal

Stem Cells, 33(7)

ISSN

1066-5099

Authors

Hashem, Sherin I

Perry, Cynthia N

Bauer, Matthieu

et al.

Publication Date

2015-07-01

DOI

10.1002/stem.2015

Peer reviewed

HHS Public Access

Author manuscript

Stem Cells. Author manuscript; available in PMC 2015 November 18.

Published in final edited form as:

Stem Cells. 2015 July ; 33(7): 2343–2350. doi:10.1002/stem.2015.

Brief Report: Oxidative Stress Mediates Cardiomyocyte Apoptosis in a Human Model of Danon Disease and Heart Failure

Sherin I. Hashem[a,†], **Cynthia N. Perry**[a,†], **Matthieu Bauer**[a], **Sangyoon Han**[a], **Stacey D. Clegg**[b], **Kunfu Ouyang**[a], **Dekker C. Deacon**[a], **Mary Spinharney**[a], **Athanasia D. Panopoulos**[c], **Juan Carlos Izpisua Belmonte**[c], **Kelly A. Frazer**[d,e], **Ju Chen**[a], **Qiuming Gong**[b], **Zhengfeng Zhou**[b], **Neil C. Chi**[a,e,*], and **Eric D. Adler**[a,*]

[a]Division of Cardiology, Department of Medicine; University of California San Diego, San Diego, California, USA

[b]Knight Cardiovascular Institute, Oregon Health Sciences University, Portland, Oregon, USA

[c]Gene Expression Laboratory, Salk Institute for Biological Studies, La Jolla, California, USA

[d]Department of Pediatrics, University of California San Diego, San Diego, California, USA

[e]Institute for Genomic Medicine, University of California San Diego, San Diego, California, USA

Abstract

Danon disease is a familial cardiomyopathy associated with impaired autophagy due to mutations in the gene encoding lysosomal-associated membrane protein type 2 (*LAMP-2*). Emerging evidence has highlighted the importance of autophagy in regulating cardiomyocyte bioenergetics, function, and survival. However, the mechanisms responsible for cellular dysfunction and death in cardiomyocytes with impaired autophagic flux remain unclear. To investigate the molecular mechanisms responsible for Danon disease, we created induced pluripotent stem cells (iPSCs) from two patients with different *LAMP-2* mutations. Danon iPSC-derived cardiomyocytes (iPSC-CMs) exhibited impaired autophagic flux and key features of heart failure such as increased cell size, increased expression of natriuretic peptides, and abnormal calcium handling compared to control iPSC-CMs. Additionally, Danon iPSC-CMs demonstrated excessive amounts of mitochondrial oxidative stress and apoptosis. Using the sulfhydryl antioxidant *N*-acetylcysteine to scavenge free radicals resulted in a significant reduction in apoptotic cell death in Danon iPSC-CMs. In summary, we have modeled Danon disease using human iPSC-CMs from patients with

Correspondence: Eric D. Adler, M.D., 9500 Gilman Drive, Leichtag Biomedical Research Building, Rm 451, La Jolla, California 92093-0613J, USA. Telephone: (858) 657-5326; Fax (858) 657-5044; eradler@ucsd.edu; or Neil C. Chi M.D., Ph.D., 9500 Gilman Drive, Leichtag Biomedical Research Building, Rm 451, La Jolla, California 92093-0613J, USA. Telephone: (858) 822-1842; Fax (858) 534-0522; nchi@ucsd.edu.

S.I.H. and C.N.P. contributed equally to this work

N.C.C. and E.D.A. contributed equally to this work.

Author Contributions

S.I.H., C.N.P., S.D.C., N.C.C., and E.D.A.: conception and design; S.I.H., C.N.P., M.B., S.H., S.D.C., K.O., D.C.D., M.S., A.D.P., J.C.I.B., Q.G., and Z.Z.: Collection and assembly of data; S.I.H., C.N.P., M.B., S.H., S.D.C., K.O., D.C.D., A.D.P., K.A.F., J.C., Q.G., Z.Z., N.C.C., and E.D.A.: data analysis and interpretation; S.I.H., C.N.P., S.D.C., N.C.C., and E.D.A.: manuscript writing; C.N.P., K.A.F., J.C., N.C.C., and E.D.A.: financial support;

Disclosure of Potential Conflicts of Interest

The authors indicate no potential conflicts of interest.

mutations in *LAMP-2*, allowing us to gain mechanistic insight into the pathogenesis of this disease. We demonstrate that LAMP-2 deficiency leads to an impairment in autophagic flux, which results in excessive oxidative stress, and subsequent cardiomyocyte apoptosis. Scavenging excessive free radicals with antioxidants may be beneficial for patients with Danon disease. In vivo studies will be necessary to validate this new treatment strategy.

Keywords

Induced pluripotent stem cells; Danon disease; Autophagy; Oxidative stress; Apoptosis

Introduction

Macroautophagy (abbreviated here as autophagy) is a highly conserved proteolytic process that begins with the sequestration of proteins and organelles by autophagosomes. Subsequently, the autophagosomes fuse with lysosomes, allowing the breakdown of the contents for cellular recycling [1, 2]. Impaired autophagy is implicated in a variety of human diseases, including heart failure, which is a leading cause of cardiovascular death [3–6].

Lysosomal-associated membrane protein type 2 (LAMP-2) is a lysosomal membrane glycoprotein that is critical for lysosome–autophagosome fusion [7]. Mutations in *LAMP-2* are associated with the X-linked disorder Danon disease [8, 9]. Danon disease patients have severe cardiac and skeletal muscle abnormalities and frequently die from heart failure in the second or third decade of life; however, the mechanisms by which loss of LAMP-2 leads to cardiac myocyte dysfunction remain unresolved. To date, no specific therapies have been identified for this deadly disease.

To gain further insight into the molecular mechanisms responsible for Danon disease, we created induced pluripotent stem cells (iPSCs) from the dermal fibroblasts of two Danon disease patients with different mutations in *LAMP-2*. We used these cells to generate Danon iPSC-derived cardiomyocytes (iPSC-CMs) to study the consequences of LAMP-2 deficiency in a human disease model.

Materials and Methods

Provided as Supporting Information.

Results and Discussion

Identification and Characterization of Two Danon Disease Patients with Distinct Mutations of *LAMP-2*

We recruited two Danon disease patients with heart failure for this study. Echocardiographic examination of the Danon patients revealed cardiac hypertrophy and reduced ejection fraction (Supporting Information Fig. 1A, B). Skeletal muscle biopsy in the first patient, Danon A, revealed large vacuoles and lysosomal accumulation within the myofibrils, which were visible by both light and electron microscopy (EM) (Supporting Information Fig. 1C–E). Genomic sequencing of the Danon A patient identified a previously undescribed 2-bp

insertion in exon 2 of the *LAMP-2* gene (129–130 insAT), which resulted in a premature termination codon 16-bp downstream (Supporting Information Fig. 2A). The second patient, Danon B, harbored a previously described single point mutation in intron 1 of the *LAMP-2* gene (IVS-1 c.64+1 G>A) [10], which lead to the retention of the first intron and subsequent alteration of splicing (Supporting Information Fig. 2B).

Next, we expanded skin fibroblasts collected from skin biopsies performed on each patient (herein called Danon skin fibroblasts). Quantitative reverse transcription polymerase chain reaction (RT-PCR) analysis performed on the Danon skin fibroblasts from both patients showed nearly complete absence of *LAMP-2* mRNA. When Danon skin fibroblasts from these patients were treated with cycloheximide, a known inhibitor of nonsense-mediated decay (NMD), *LAMP-2* mRNA expression levels increased suggesting that the mutant mRNA is targeted by NMD (Supporting Information Fig. 2C). Consistent with these findings, LAMP-2 protein was absent in the Danon skin fibroblasts from both patients (Supporting Information Fig. 2D–F, J).

Given the role of LAMP-2 in lysosome-autophagosome fusion [7], we performed EM on the Danon skin fibroblasts to determine if the absence of LAMP-2 would lead to the accumulation of intracytoplasmic vacuoles. Danon skin fibroblasts had significantly more autophagic vacuoles (AVs) and lysosomes than wild-type (WT) fibroblasts (Supporting Information Fig. 2G–I, K) ($p<0.001$ vs. WT), suggesting a defect in the final steps of autophagic flux. To further validate this conclusion, we used a previously described tandem fluorescent mRFP-GFP-LC3B fusion BacMam reporter to transduce Danon and WT skin fibroblasts [11, 12]. GFP-LC3 loses fluorescence, when exposed to lysosomal acidity, whereas mRFP-LC3 does not. Hence, mRFP labels AVs both before (early AVs) and after (mature AVs) fusion with lysosomes, whereas GFP labels AVs only before fusion with lysosomes (early AVs) (Supporting Information Fig. 3A). Our data demonstrates that Danon skin fibroblasts contained significantly more early AVs than WT, and were nearly devoid of mature AVs (Supporting Information Fig. 3B–E) ($p < 0.001$). These results indicate that Danon skin fibroblasts fail to complete autophagosome–lysosome fusion. To determine whether Danon skin fibroblasts could increase autophagic flux despite the absence of LAMP-2, we used two different methods to induce autophagy: (a) treating cells with rapamycin, a known inducer of autophagy, or (b) depriving them of nutrients for 4 hours [13]. Rapamycin increased the formation of early AVs in both Danon and WT fibroblasts, but starvation did not (Supporting Information Fig. 3E) suggesting that human dermal fibroblasts are relatively insensitive to starvation-induced autophagy.

Danon iPSC-CMs Exhibit Impaired Autophagosome Maturation

To investigate the effect of *LAMP-2* mutations in cardiomyocytes, a cell type commonly affected by Danon disease, we created five independent Danon patient-derived iPSC lines from the two Danon disease patients: three independent clones generated from patient A (clones A1–3) and two independent clones from patient B (clones B1–2) (Supporting Information Fig. 4). We compared these five lines with two wild-type (WT1–2) iPSC lines derived from unrelated individuals without cardiovascular disease and with normal expression of *LAMP-2* (Supporting Information Fig. 5A). We also generated a stable Danon

A2 iPSC line overexpressing human *LAMP-2B* (NM_013995.2) under the regulation of doxycycline (*LAMP-2 OE*) (Supporting Information Fig. 6). We chose LAMP-2B because all mutations reported in Danon disease affect the LAMP-2B isoform [14]. Furthermore, LAMP-2B is the isoform most abundantly expressed in cardiac and skeletal muscle, which are the tissues primarily affected in Danon disease [15]. The Danon and WT iPSC lines all generated cardiomyocytes with high cardiac differentiation efficiency and with no significant difference between the lines (Supporting Information Fig. 4H).

WT and Danon iPSC-CMs from all lines expressed the cardiac-specific contractile protein α-actinin (Fig. 1E–H, Supporting Information Fig. 5A), but Danon iPSC-CMs contained no detectable LAMP-2 protein (Fig. 1B, C, F, G; Supporting Information Fig. 5A). Upon doxycycline treatment, *LAMP-2* expression was observed in *LAMP-2 OE* iPSC-CMs (Fig. 1D, H) and showed an increase in a dose–responsive manner (Supporting Information Fig. 6). EM analysis revealed that Danon iPSC-CMs had significantly more total AVs and lysosomes than WT iPSC-CMs (Fig. 1I–K, M) ($p<0.01$). Moreover, while WT iPSC-CMs showed elongated mitochondria that were aligned parallel to assembling myofibrils, mitochondria in Danon iPSCCMs derived from both Danon patients appeared rounded and were significantly fragmented (Fig. 1I–K, N) ($p<0.001$). *LAMP-2 OE* iPSC-CMs exhibited a decrease in the number of total AVs (Fig. 1L, M) ($p<0.01$) and a reduction in mitochondrial fragmentation (Fig. 1L, N) ($p<0.01$) compared to Danon A2 iPSC-CMs. Next, we evaluated autophagic flux using the tandem mRFP-GFP-LC3B reporter in the iPSC-CMs lines. Danon iPSC-CMs had significantly more early AVs and displayed a nearly complete absence of mature AVs (Fig. 2A–C, E, Supporting Information Fig. 5B). Early AV levels were not significantly different between the Danon iPSC-CM lines. Furthermore, Danon iPSC-CMs exhibited significantly higher levels of microtubule-associated protein 1 light chain 3-II (LC3-II) compared to WT iPSC-CMs under basal culture conditions (Fig. 2F, G) ($p<0.01$). LC3-II associates with autophagosome membranes and is readily degraded by lysosomal enzymes upon autophagosome–lysosomes fusion [16]. The increased levels of LC3-II in Danon iPSC-CMs suggest a defect in autophagic flux. Importantly, unlike dermal fibroblasts (Supporting Information Fig. 3E and 7A, B), both Danon and WT iPSC-CMs showed an increase in LC3-II levels as well as an increase in the number of early AVs when starved (Supporting Information Fig. 7C–E), indicating that iPSC-CMs are sensitive to starvation-induced autophagy. This may explain why this disease preferentially affects metabolically active cell types such as cardiac and skeletal myocytes.

LAMP-2 OE iPSC-CMs exhibited an increase in the number of mature AVs (Fig. 2D, E) ($p<0.01$) and a reduction in LC3-II levels (Fig. 2H, I, Supporting Information Fig. 7C, D) ($p<0.01$) compared to Danon A2 iPSC-CMs indicating that reintroduction of *LAMP-2* could rescue autophagic maturation. These data confirm that Danon iPSC-CMs exhibit defective autophagic flux compared to WT iPSC-CMs, and that this defect could be rescued by restoring *LAMP-2* expression.

Danon iPSC-CMs Exhibit Key Features of Heart Failure In Vitro

Next, we examined the size, gene expression, and function of Danon iPSC-CMs to determine whether they recapitulated the heart failure phenotype observed in Danon

patients. Cytological analysis revealed that Danon iPSC-CMs from all lines were significantly larger than WT iPSC-CMs, phenocopying the hypertrophy observed in Danon patients (Fig. 3A–E) (p <0.05) [17].

Atrial Natriuretic Peptide (ANP) and Brain Natriuretic Peptide (BNP) are two hormones synthesized by cardiomyocytes in response to stress [18]. Expression of both ANP and BNP was markedly increased in all Danon iPSC-CMs lines compared to WT cells, akin to the induction seen in cardiomyopathies such as Danon disease (Fig. 3F) (p<0.05 for ANP; p<0.01 for BNP). Induction of *LAMP-2* in the *LAMP-2 OE* iPSC-CMs restored cell size and natriuretic peptide expression to near WT levels (Fig. 3D–F), confirming that *LAMP-2* was responsible for the stress-related phenotype observed in Danon iPSC-CM.

Because many studies have shown altered Ca^{2+} cycling and handling in heart failure [19], we analyzed Ca^{2+} handling properties in our iPSC-derived CMs at baseline and under adrenergic receptor stimulation. Calcium kinetics were measured using the Ca^{2+}-sensitive fluorescent dye Fluo-4-AM. As expected, iPSC-CMs from Danon A2, Danon B2, WT2, and *LAMP-2OE* lines exhibited shorter calcium decay times (τ) when exposed to isoproterenol-mediated β-adrenergic receptor activation compared to baseline (Fig. 3G, Supporting Information Fig. 8B). However, Danon A2 and B2 iPSC-CMs consistently exhibited longer calcium decay times compared to WT2 iPSC-CMs under all conditions examined (Fig. 3G, Supporting Information Fig. 8A, B), consistent with the decline in systolic and diastolic function observed in heart failure [20, 21]. This is in concordance with prior investigations of other iPSC-CMs from patients with cardiomyopathies [22, 23], and with previous reports of cardiomyocytes isolated from human patients with heart failure [19]. *LAMP-2 OE* iPSC-CMs showed calcium decay times near WT levels, indicating a rescue of the pathophysiologic phenotype (Fig. 3G, Supporting Information Fig. 8B). Taken together, these pathologic cellular, molecular, and functional changes in Danon iPSC-CMs recapitulate to some extent the clinical heart failure phenotype seen in patients with Danon disease [8, 17].

Danon iPSC-CMs Exhibit Abnormal Levels of Oxidative Stress and Apoptosis

Mitochondrial integrity and turnover play a pivotal role in cardiomyocyte bioenergetics and function [24, 25]. Given the critical role of autophagy in maintaining mitochondrial homeostasis [25, 26], we further investigated mitochondrial structure and function in the Danon iPSC-CMs. We transduced iPSC-CMs with BacMam mito-GFP, which readily labels mitochondria. In WT iPSC-CMs, unfragmented, elongated mitochondrial networks were observed (Supporting Information Fig. 9A), whereas Danon iPSC-CMs contained short, fragmented mitochondria with a poor mitochondrial network (Supporting Information Fig. 9B,C). This finding was further validated with EM, which revealed the accumulation of fragmented mitochondria in the cytoplasm and within autophagosomes in Danon iPSC-CMs (Fig. 1I–K, N, Supporting Information Fig. 9D, E, G) (p<0.001).

Previous studies have indicated that undigested material within the autophagosome, including dysfunctional mitochondria, may be a source of free radicals that could result in AV leakage, cellular dysfunction, and apoptosis [26–30]. Given the abnormal mitochondria observed in the Danon iPSC-CMs, we examined whether there were abnormal levels of

oxidative stress and apoptosis in these cells. Danon iPSC-CMs from all lines displayed markedly higher TUNEL staining than WT control lines (Fig. 4A–E, Supporting Information Fig. 5C) ($p<0.05$) suggesting increased apoptosis in Danon cells. In addition, Danon iPSC-CMs had significantly higher levels of total oxidative stress than WT controls, as measured using 2′-7′-dichlorodihydrofluorescein diacetate (CM-H_2DCFDA) (Fig. 4F) ($p<0.05$ for Danon A; $p<0.01$ for Danon B vs. WT baseline) [31]. Induction of *LAMP-2* expression in the *LAMP-2 OE* iPSC-CMs significantly decreased the abnormal level of reactive oxygen species (ROS) (Fig. 4F) ($p<0.01$).

Given these findings, we hypothesized that the apoptosis observed in Danon iPSC-CMs was due to the high levels of oxidative stress detected in these cells. Thus, we treated Danon iPSC-CMs with the potent antioxidant *N*-acetylcysteine (NAC). Danon iPSC-CMs treated with 5 mM NAC demonstrated a significant reduction in total ROS levels compared to untreated Danon cells (Fig. 4F) ($p<0.01$ vs. Danon A baseline; $p<0.05$ vs. Danon B baseline). Treating the Danon cells with rotenone, a mitochondrial complex I inhibitor, reduced ROS production indicating that the majority of ROS was generated by mitochondria [32]. Furthermore, mitochondrial superoxide production (mitochondrial oxidative stress [mROS]), measured using mitoSOX red, was significantly elevated in Danon iPSCCMs (Fig. 4G) ($p<0.05$). These elevated levels of mROS were significantly reduced by NAC and rotenone, as well as by doxycycline-induced *LAMP-2* overexpression (Fig. 4G) ($p<0.01$). Induction of *LAMP-2* in *LAMP-2 OE* iPSC-CMs significantly decreased the number of fragmented mitochondria (Fig. 1L, N, Supporting Information Fig. 9D, I) ($p<0.001$), as well as the number of AVs (Fig. 1L, M, Supporting Information Fig. 9I). Danon iPSC-CMs treated with NAC showed elongated mitochondria, and a significant decrease in mitochondria fragmentation despite the continued accumulation of AVs (Supporting Information Fig. 9D, F, H). This data suggests that oxidative stress plays a role in the observed mitochondrial fragmentation. Importantly, treatment with NAC reversed the increased apoptotic cell death observed in Danon iPSC-CMs (Fig. 4E) ($p<0.05$ for Danon A; $p<0.01$ for Danon B), supporting a causal relationship between oxidative stress and apoptosis. However, the abnormal calcium handling was not corrected with NAC treatment (Supporting Information Fig. 8B, C) suggesting that the altered calcium dynamics may be due to mechanisms other than oxidative stress. It is also possible that the residual damaged mitochondria due to impaired mitophagy results in dysfunctional mitochondrial calcium homeostasis. Nonetheless, the antiapoptotic and antioxidant effects of NAC may be of significant benefit to Danon disease patients given that postmortem examination of affected hearts shows significant myocardial necrosis and fibrosis [33]. This new treatment strategy should be further validated using in vivo models.

Conclusions

We identified two Danon patients with distinct *LAMP-2* mutations that lead to a complete absence of LAMP-2 protein, which results in impaired autophagosome–lysosome fusion, leading to defective autophagic flux. Using multiple iPSC lines from these patients, we created a novel in vitro human model of Danon disease and demonstrated that impaired autophagy results in increased oxidative stress and subsequent apoptosis in Danon cells. These data provide insight into the cellular and molecular defects underlying the

pathogenesis of end stage heart failure in Danon disease. Furthermore, we show that scavenging free radicals and relieving excessive oxidative stress with the clinically approved agent NAC prevents pathologic apoptotic cell death in Danon iPSCCMs in vitro. These findings suggest that treating Danon patients with antioxidants such as NAC may be useful for mitigating the disease. Elucidating the mechanisms by which impaired autophagy leads to cell death in cardiac myocytes may also assist in the development of novel treatments for a plethora of other diseases associated with impaired autophagic flux.

Supplementary Material

Refer to Web version on PubMed Central for supplementary material.

Acknowledgments

We thank Adler and Chi lab members for their support and intellectual and editorial feedback during this project. We also thank the UCSD CMM EM facility for preparation of EM slides, OHSU for preparation and histological analysis of patient biopsies, Life Technologies for the generous gift of the Premo tandem mRFP-GFP-LC3B BacMam reporter system, and Steven Kattman and Robert Ross for feedback on the manuscript. This research was funded by grants from the National Institutes of Health and the California Institute of Regenerative Medicine (CIRM): 7K23HL107755 and CIRM TR305687 for E.D.A., F32 HL116068 for C.N.P., R01 HL68854 for Z.Z., DP2OD007464 for N.C.C., and U01HL107442 for J.C.I.B., K.A.F., and N.C.C. K.O. was supported by the National Key Basic Research Program of China (2013CB531200) and the National Science Foundation of China (31370823, 91439130). Work in the laboratory of JCIB was supported by The Leona M. and Harry B. Helmsley Charitable Foundation. C.N.P. is currently affiliated with Department of Medical Education, Paul L. Foster School of Medicine, Texas Tech University Health Sciences Center, El Paso, TX; S.D.C. is currently affiliated with Division of Cardiology, University of New Mexico Health Science Center, Albuquerque, NM; K.O. is currently affiliated with School of Chemical Biology and Biotechnology, Peking University, Shenzhen 518055, People's Republic of China; A.D.P. is currently affiliated with Department of Biological Sciences, University of Notre Dame, Notre Dame, IN.

References

1. He C, Klionsky DJ. Regulation mechanisms and signaling pathways of autophagy. Annu Rev Genet. 2009; 43:67–93. [PubMed: 19653858]
2. Singh R, Cuervo AM. Autophagy in the cellular energetic balance. Cell Metab. 2011; 13:495–504. [PubMed: 21531332]
3. Gonzalez CD, Lee MS, Marchetti P, et al. The emerging role of autophagy in the pathophysiology of diabetes mellitus. Autophagy. 2011; 7:2–11. [PubMed: 20935516]
4. Choi AM, Ryter SW, Levine B. Autophagy in human health and disease. N Engl J Med. 2013; 368:651–662. [PubMed: 23406030]
5. Gustafsson AB, Gottlieb RA. Autophagy in ischemic heart disease. Circ Res. 2009; 104:150–158. [PubMed: 19179668]
6. De Meyer GR, De Keulenaer GW, Martinet W. Role of autophagy in heart failure associated with aging. Heart Fail Rev. 2010; 15:423–430. [PubMed: 20383579]
7. Eskelinen EL, Illert AL, Tanaka Y, et al. Role of LAMP-2 in lysosome biogenesis and autophagy. Mol Biol Cell. 2002; 13:3355–3368. [PubMed: 12221139]
8. Maron BJ, Roberts WC, Arad M, et al. Clinical outcome and phenotypic expression in LAMP2 cardiomyopathy. JAMA. 2009; 301:1253–1259. [PubMed: 19318653]
9. Nishino I, Fu J, Tanji K, et al. Primary LAMP-2 deficiency causes X-linked vacuolar cardiomyopathy and myopathy (Danon disease). Nature. 2000; 406:906–910. [PubMed: 10972294]
10. Boucek D, Jirikowic J, Taylor M. Natural history of Danon disease. Genet Med. 2011; 13:563–568. [PubMed: 21415759]

11. Kimura S, Noda T, Yoshimori T. Dissection of the autophagosome maturation process by a novel reporter protein, tandem fluorescent-tagged LC3. Autophagy. 2007; 3:452–460. [PubMed: 17534139]
12. Tanida I, Ueno T, Kominami E. LC3 conjugation system in mammalian autophagy. Int J Biochem Cell Biol. 2004; 36:2503–2518. [PubMed: 15325588]
13. Tasdemir E, Galluzzi L, Maiuri MC, et al. Methods for assessing autophagy and autophagic cell death. Autophagosome and phagosome. Methods Mol Biol. 2008; 445:29–76. [PubMed: 18425442]
14. D'souza RS, Levandowski C, Slavov D, et al. Danon disease: Clinical features, evaluation, and management. Circ: Heart Fail. 2014; 7:843–849. [PubMed: 25228319]
15. Konecki DS, Foetisch K, Zimmer KP, et al. An alternatively spliced form of the human lysosome-associated membrane protein-2 gene is expressed in a tissue-specific manner. Biochem Biophys Res Commun. 1995; 215:757–767. [PubMed: 7488019]
16. Tanida I, Ueno T, Kominami E. LC3 and autophagy. Methods Mol Biol. 2008; 445:77–88. [PubMed: 18425443]
17. Yang Z, McMahon CJ, Smith LR, et al. Danon disease as an underrecognized cause of hypertrophic cardiomyopathy in children. Circ Res. 2005; 112:1612–1617.
18. Langenickel T, Pagel I, Höhnel K, et al. Differential regulation of cardiac ANP and BNP mRNA in different stages of experimental heart failure. Am J Physiol Heart Circ Physiol. 2000; 278:H1500–H1506. [PubMed: 10775127]
19. Yano M, Ikeda Y, Matsuzaki M. Altered intracellular Ca^{2+} handling in heart failure. J Clin Invest. 2005; 115:556–564. [PubMed: 15765137]
20. Dhalla NS, Das PK, Sharma GP. Subcellular basis of cardiac contractile failure. J Mol Cell Cardiol. 1978; 10:363–385. [PubMed: 205659]
21. Ito Y, Suko J, Chidsey CA. Intracellular calcium and myocardial contractility. V. Calcium uptake of sarcoplasmic reticulum fractions in hypertrophied and failing rabbit hearts. J Mol Cell Cardiol. 1974; 6:237–247. [PubMed: 4837895]
22. Sun N, Yazawa M, Liu J, et al. Patient-specific induced pluripotent stem cells as a model for familial dilated cardiomyopathy. Sci Transl Med. 2012; 4:130ra47.
23. Carvajal-Vergara X, Sevilla A, D'Souza SL, et al. Patient-specific induced pluripotent stem-cell-derived models of LEOPARD syndrome. Nature. 2010; 465:808–812. [PubMed: 20535210]
24. Chen L, Knowlton AA. Mitochondrial dynamics in heart failure. Congest Heart Fail. 2011; 17:257–261. [PubMed: 22848903]
25. Kubli DA, Gustafsson AB. Mitochondria and mitophagy: The yin and yang of cell death control. Circ Res. 2012; 111:1208–1221. [PubMed: 23065344]
26. Kim I, Rodriguez-Enriquez S, Lemasters JJ. Selective degradation of mitochondria by mitophagy. Arch Biochem Biophys. 2007; 462:245–253. [PubMed: 17475204]
27. Wu JJ, Quijano C, Chen E, et al. Mitochondrial dysfunction and oxidative stress mediate the physiological impairment induced by the disruption of autophagy. Aging (Albany NY). 2009; 1:425–437. [PubMed: 20157526]
28. Yang J, Wu LJ, Tashino S, et al. Reactive oxygen species and nitric oxide regulate mitochondria-dependent apoptosis and autophagy in evodiamine-treated human cervix carcinoma HeLa cells. Free Radic Res. 2008; 42:492–504. [PubMed: 18484413]
29. Kussmaul L, Hirst J. The mechanism of superoxide production by NADH:ubiquinone oxidoreductase (complex I) from bovine heart mitochondria. Proc Natl Acad Sci USA. 2006; 103:7607–7612. [PubMed: 16682634]
30. Wohlgemuth SE, Calvani R, Marzetti E. The interplay between autophagy and mitochondrial dysfunction in oxidative stress-induced cardiac aging and pathology. J Mol Cell Cardiol. 2014; 71C:62–70. [PubMed: 24650874]
31. Palomero J, Pye D, Kabayo T, et al. In situ detection and measurement of intracellular reactive oxygen species in single isolated mature skeletal muscle fibers by real time fluorescence microscopy. Antioxid Redox Signal. 2008; 10:1463–1474. [PubMed: 18407749]

32. Duan Y, Gross RA, Sheu SS. Ca^{2+}-dependent generation of mitochondrial reactive oxygen species serves as a signal for poly (ADP-ribose) polymerase-1 activation during glutamate excitotoxicity. J Physiol. 2007; 585(Pt 3):741–758. [PubMed: 17947304]

33. Balmer C, Ballhausen D, Bosshard NU, et al. Familial x-linked cardiomyopathy (danon disease): Diagnostic confirmation by mutation analysis of the lamp2gene. Eur J Pediatr. 2005; 164:509–514. [PubMed: 15889279]

34. Hansen TE, Johansen T. Following autophagy step by step. BMC Biol. 2011; 9:39. [PubMed: 21635796]

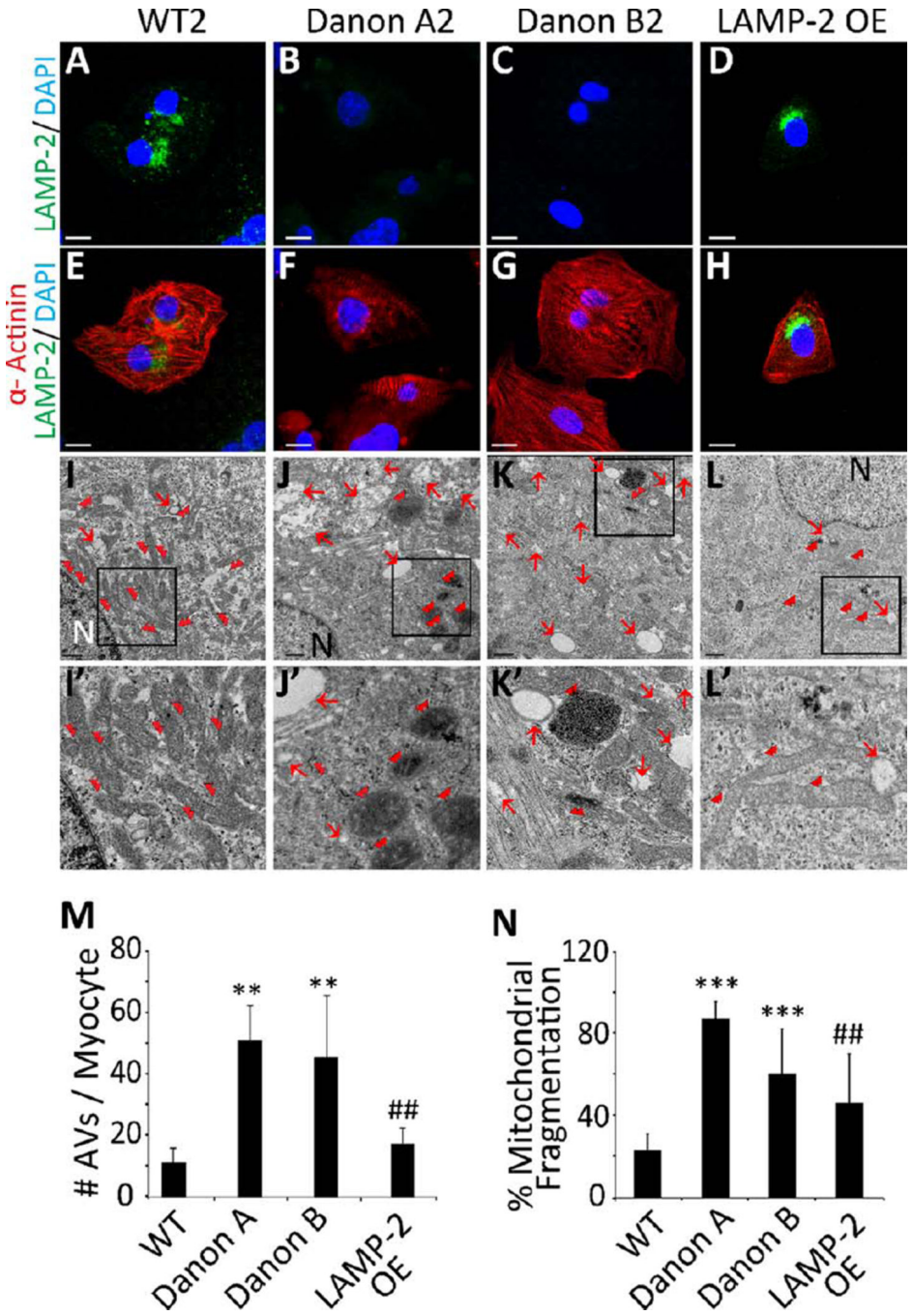

Figure 1.

LAMP-2 deficient induced pluripotent stem cell-derived cardiomyocytes (iPSC-CMs) exhibit accumulation of AVs and mitochondrial fragmentation. **(A–H)**: Representative confocal images of iPSC-CMs from (A,E) WT2, (B,F) Danon A2, (C,G) Danon B2, and (D,H) *LAMP-2 OE* lines immunostained for LAMP-2 (green) and sarcomeric α-actinin (red) reveal no visible LAMP-2 in Danon iPSC-CMs. *LAMP-2 OE* iPSC-CMs show LAMP-2 protein expression. DAPI (blue) was used for nuclear counterstaining. Scale bar = 10 μm. **(I–L)**: Electron microscopy (EM) of iPSC-CMs from (I) WT2, (J) Danon A2, (K) Danon

B2, and (L) *LAMP-2 OE* lines reveals significant accumulation of intracytoplasmic vacuoles (red arrows) and presence of round fragmented mitochondria (red double arrowheads) in Danon iPSC-CMs. A reduction in the number of intracytoplasmic vacuoles and the presence of elongated mitochondria are noted in *LAMP-2 OE* compared to Danon A2 iPSC-CMs. N: nucleus. Scale bar = 0.5 μm. **(I′–L′)**: Enlarged image of the boxed area in I–L. **(M)**: Quantification of AVs visualized by EM reveals the accumulation of more AVs in the Danon A1–3 (45.9±9.9 AVs/CM) and Danon B1–2 (40.15±17.6 AVs/CM) iPSC-CM lines compared to WT1–2 (10.3±3.4 AVs/CM) and *LAMP-2 OE* (18.6±3.5 AVs/CM) iPSC-CM lines. **, $p<.01$ vs. WT; ##, $p<.01$ vs. Danon A, Student's *t* test, $n = 3$. **(N)**: Quantification of mitochondrial fragmentation visualized by EM reveals the presence of a high percentage of fragmented mitochondria in Danon A and Danon B compared to WT and *LAMP-2 OE* iPSC-CM lines (% mitochondrial fragmentation is 87.4±8.5 for Danon A1–3, 60.6±22.1 for Danon B1–2, vs. 23.5±7.8 for WT1–2, and 46.5±23.9 for *LAMP-2 OE* iPSC-CMs). ***, $p<.001$ vs. WT; ##, $p<.01$ vs. Danon A, Student's *t* test, $n = 3$. Data are the means±SD. Abbreviations: AVs, autophagic vacuoles; DAPI, 4′,6-diamidino-2-phenylindole; EM, electron microscopy; *LAMP-2*, lysosomal-associated membrane protein type 2; WT, wild-type

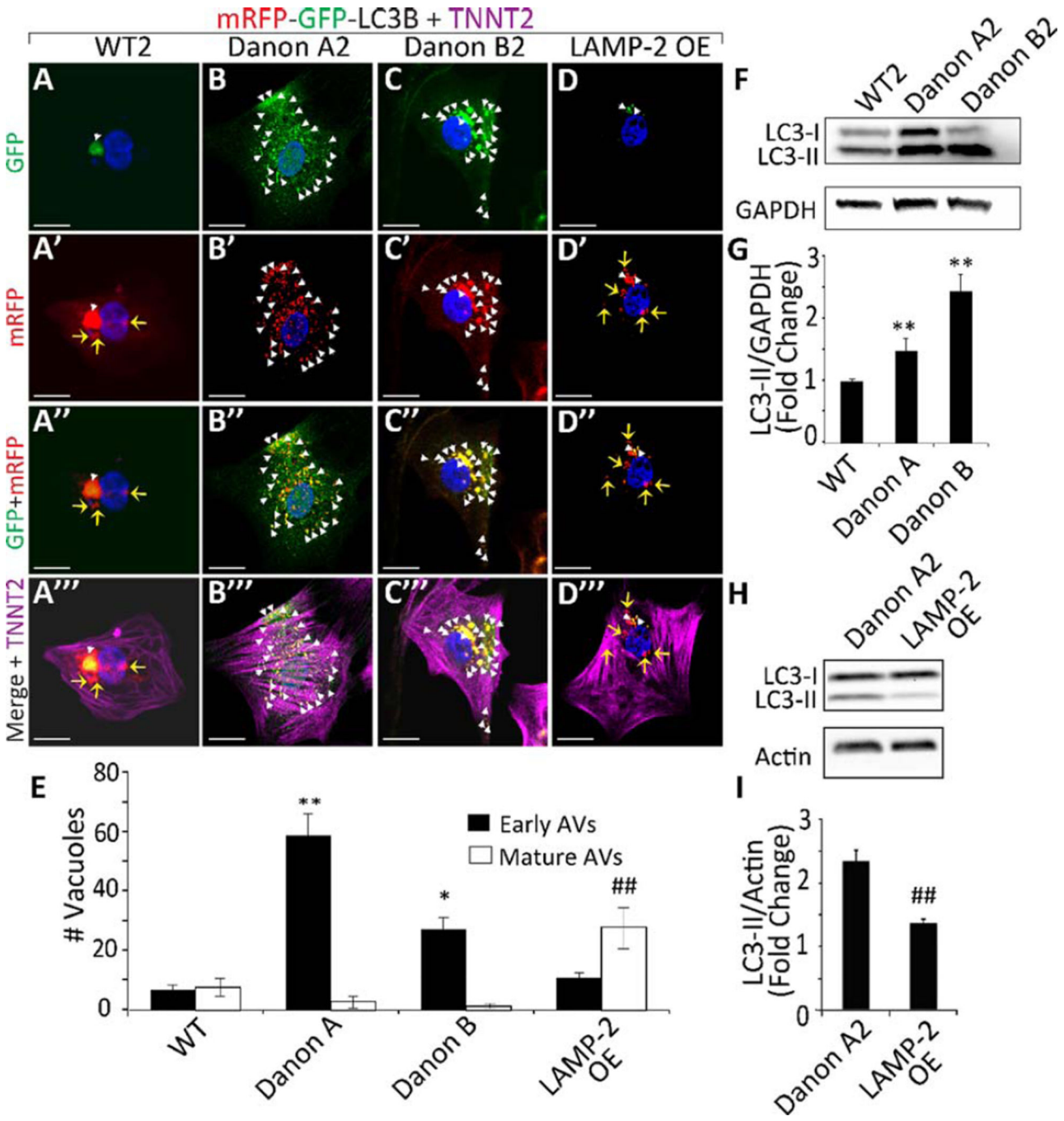

Figure 2.

LAMP-2 deficient induced pluripotent stem cell-derived cardiomyocytes (iPSC-CMs) exhibit impaired autophagic flux. **(A–D″′)**: Confocal images of iPSC-CMs from (A–A″′) WT2, (B–B‴) Danon A2, (C–C″′) Danon B2, and (D–D″′) *LAMP-2 OE* lines expressing tandem fluorescent mRFP-GFP-LC3B (tf-LC3B). GFP is quenched upon autophagosome–lysosome fusion, whereas mRFP remains stable. Early autophagic vacuoles (AVs, white arrowheads) express both mRFP and GFP signals, whereas mature AVs (yellow arrows) express the mRFP signal only. **(A–D)**: Images show GFP signal, that is, early AVs. **(A′–D′)**:

Images show mRFP signal, that is, early and mature AVs. **(A″ –D″)**: Images show colocalization of GFP and mRFP signals of the tf–LC3B. **(A″′–D″′)**: Images show cardiac troponin T (TNNT2: magenta) immunostaining of the cells expressing tf-LC3B. DAPI (blue) was used to counterstain nuclei. Scale bar = 10 μm. **(E)**: Quantification of early and mature AVs in WT, Danon A, Danon B, and *LAMP-2 OE* iPSC-CMs expressing tfLC3B reveals that Danon iPSC-CMs exhibit an increase in early AVs (59±13.1 for Danon A1–3, 29.5±6.8 for Danon B1–2 vs. 7±2.3 for WT1–2 iPSC-CM lines) and a reduction in mature AVs compared to WT lines (3.0±2.3 for Danon A1–3, 1.4±0.8 for Danon B1–2 vs. 7.8±3 for WT1–2 iPSC-CM lines). *LAMP-2 OE* iPSC-CMs show restored AV maturation (mature AVs 28.7±7). *, $p<.05$ vs. WT, **, $p<.01$ vs. WT; ##, $p<.01$ vs. Danon A, Student's *t* test, $n = 3$. **(F)**: Western blot of LC3-I and -II expression in WT2, Danon A2, and Danon B2 iPSC-CMs. GAPDH loading control is shown. **(G)**: Western blot quantification demonstrates significantly more LC3-II in Danon A1–3 and Danon B1–2 iPSC-CMs compared to WT1–2 lines. Results for each group are pooled from experiments performed on all clones. **, $p<.01$ vs. WT, Student's *t* test, $n = 4$. **(H)**: Western blot of LC3-I and -II expression in Danon A2 and *LAMP-2 OE* iPSC-CMs. Actin loading control is shown. **(I)**: Western blot quantification demonstrates significantly less LC3-II in *LAMP-2 OE* iPSC-CMs compared to Danon A2 line. ##, $p<.01$ vs. Danon A2, Student's *t* test, $n = 4$. Data are the means±SD. Abbreviations: AVs, autophagic vacuoles; GADPH, glyceraldehyde 3-phosphate dehydrogenase; GFP, green fluorescent protein; *LAMP-2*, lysosomal-associated membrane protein type 2; LC3, Microtubule-associated protein 1 light chain 3; mRFP, monomeric red fluorescent protein

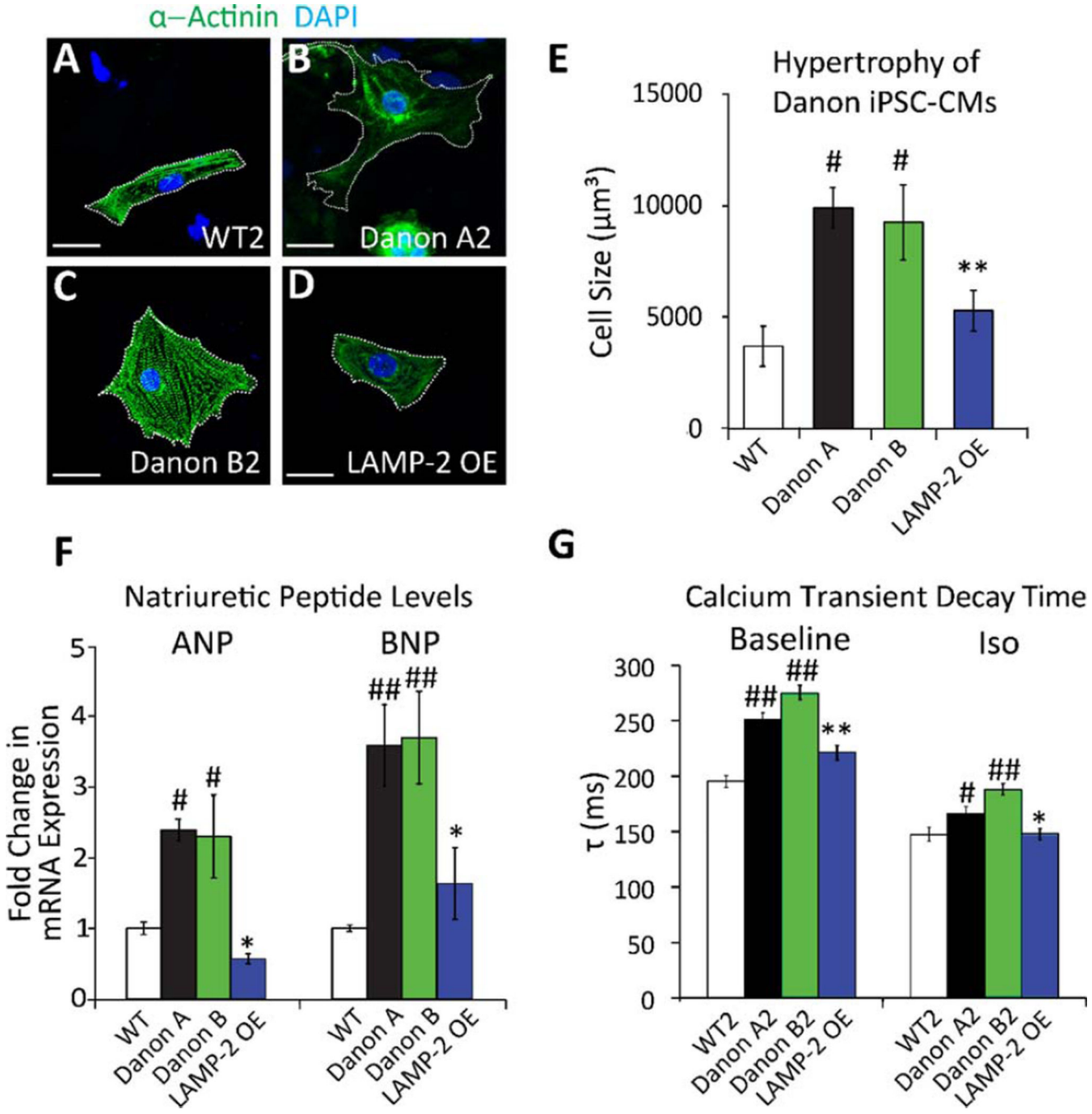

Figure 3.

Danon induced pluripotent stem cell-derived cardiomyocytes (IPSC-CMs) demonstrate increased cell size, altered gene expression, and impaired calcium reuptake. **(A–D)**: Representative confocal images of iPSC-CMs from (A) WT2, (B) Danon A2, (C) Danon B2, and (D) *LAMP-2 OE* lines immunostained for sarcomeric α-actinin (green). The cell perimeter is outlined by a white dotted line. Nuclei are counterstained with DAPI (blue). Scale bar = 20 μm. **(E)**: Danon A and B iPSC-CMs are significantly larger than WT and *LAMP-2 OE* iPSC-CMs (9,879±904 μm^3 for Danon A1–3 lines, 9,231.9±1,670 μm^3 for

Danon B1–2 lines vs. 3,694±894 μm^3 for WT1–2 lines, and 5,281±783 μm^3 for *LAMP-2 OE* line). #, $p<.05$ vs. WT; **, $p<.01$ vs. Danon A, Student's *t* test, $n = 4$. **(F)**: ANP and BNP mRNA expression levels in iPSC-CMs. Danon A1–3 and B1–2 lines express significantly more ANP and BNP than WT1–2 lines and *LAMP-2 OE* line (2.4±0.1- and 3.5±0.6-fold increase in ANP and BNP, respectively, for Danon A1–3 lines; 2.3±0.6- and 3.7±0.7-fold for Danon B1–2 lines; 0.6±0.01- and 1.6±0.5-fold for *LAMP-2 OE* line compared to WT1–2 lines). #, $p<.05$ vs. WT; ##, $p<.01$ vs. WT; *, $p<.05$ vs. Danon A, Student's *t* test, $n = 3$. **(G)**: Calcium transients were recorded in contracting cultures at baseline and after treatment with isoproterenol (Iso, 1 μM), and τ was measured. Addition of isoproterenol shortened τ compared to baseline in all lines. Danon A2 and B2 iPSC-CMs exhibit a significantly longer τ than WT2 and LAMP-2 OE lines, reflecting a slower Ca^{2+} decay rate under all conditions examined (251±6.2 ms in Danon A2 and 274.9±7.2 ms in Danon B2 vs. 195.3±5.2 ms in WT2 and 221.8±6 ms in *LAMP-2 OE* at baseline; 166.1±6.7 ms in Danon A2 and 187.8±5.8 ms in Danon B2 vs. 147.5±6.3 ms in WT2 and 148.3±4.9 ms in *LAMP-2 OE* following Iso treatment). #, $p<.05$ vs. WT, ##, $p<.01$ vs. WT, *, $p<.05$ vs. Danon A, *, $p<.01$ vs. Danon A, Student's *t* test, $n = 60$. Data are expressed as means±SD, or±SEM for calcium imaging. Abbreviations: ANP, atrial natriuretic peptide; BNP, brain natriuretic peptide; DAPI, 4′,6-diamidino-2-phenylindole; *LAMP-2*, lysosomal-associated membrane protein type 2; WT, wild-type

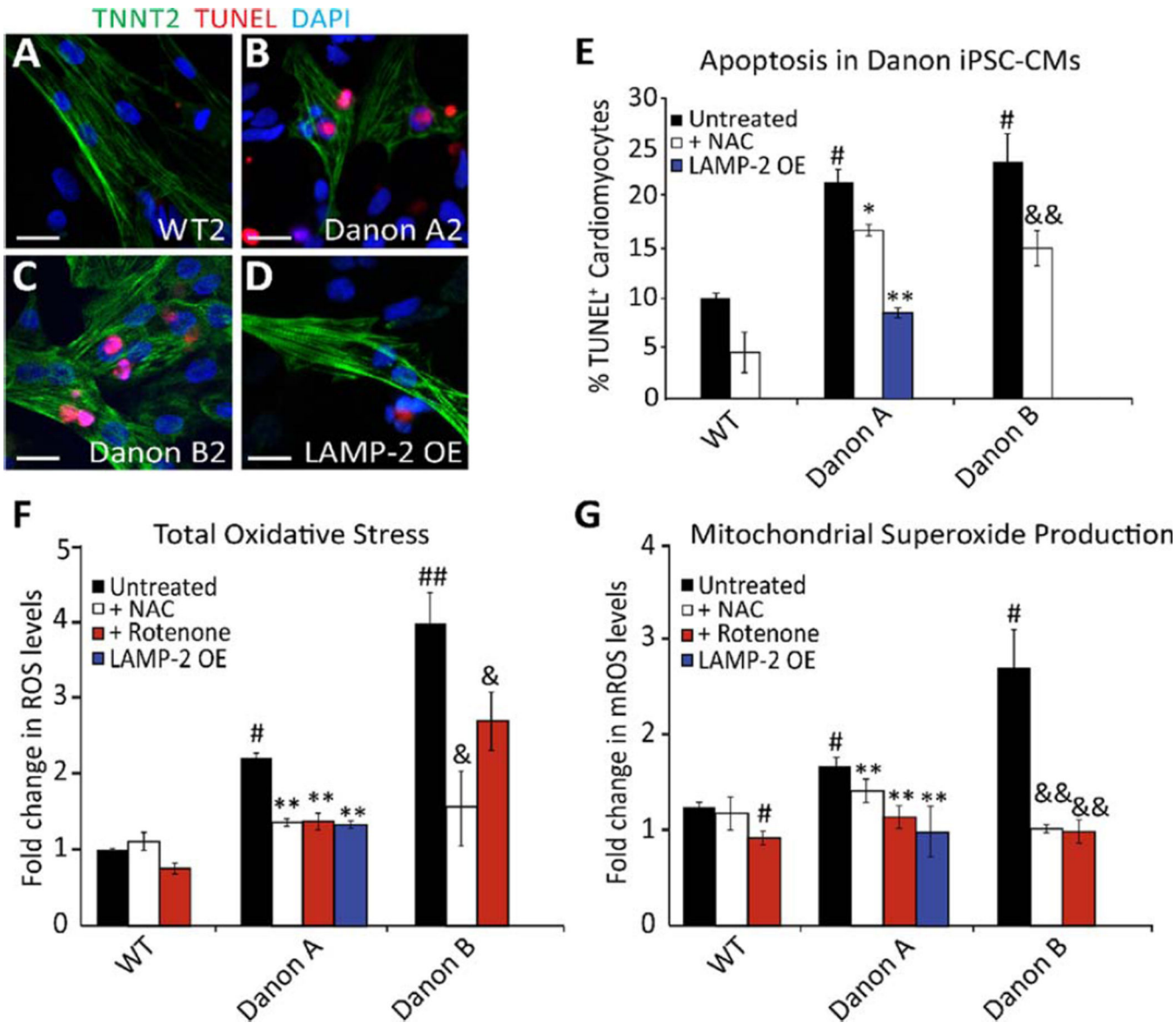

Figure 4.

LAMP-2 deficiency leads to increased cell death and mitochondrial oxidative stress (mROS). **(A–D)**: Representative confocal images of iPSC-CMs from (A) WT2, (B) Danon A2, (C) Danon B2, and (D) *LAMP-2 OE* lines immunostained for TNNT2 (green) and TUNEL (red). Nuclei are counterstained with DAPI (blue). Scale bar = 20 μm. **(E)**: Danon lines display significantly more TUNEL positive iPSCCMs than WT lines and *LAMP-2 OE* line (% $TUNEL^+$ cardiomyocytes is 21.95±1.3 for Danon A1–3 lines, 24±2.82 for Danon B1–2 lines vs. 10.15±0.57 for WT1–2 lines and 8.7±0.5 for *LAMP-2 OE* line). NAC treatment significantly reduces the number of TUNEL positive Danon iPSC-CMs (17.07 ± 0.59 for Danon A1–3 +NAC, and 15.25 ± 1.75 for Danon B1–2 +NAC). #, $p<.05$ vs. WT, *, $p<.05$ vs. Danon A, **, $p<.01$ vs. Danon A, &, $p<.01$ vs. Danon B, Student's *t* test, $n = 3$. **(F)**: iPSC-CMs from Danon A and B lines display increased levels of total ROS compared to WT and *LAMP-2 OE* lines, as measured using DCFDA (2.2±0.1-fold change for Danon

A1–3 lines, 3.97±0.7-fold for Danon B1–2 lines, and 1.33±0.1-fold for *LAMP2-OE* line compared to WT1–2 lines). #, $p<.05$ vs. WT, ##, $p<.01$ vs. WT, **, $p<.01$ vs. Danon A, &, $p<.05$ vs. Danon B, Student's *t* test, $n = 3$. **(G)**: iPSC-CMs from Danon A and B lines show increased levels of mROS compared to WT and *LAMP-2 OE* lines, as measured using mitoSOX (1.8±0.1-fold change for Danon A1–3 lines, 2.83±0.6-fold for Danon B1–2 lines, and 1.1±0.3-fold for *LAMP2-OE* line compared to WT1–2 lines). #, $p<.05$ vs. WT, **, $p<.01$ vs. Danon A, &, $p<.01$ vs. Danon B, Student's *t* test, $n = 3$. Data are expressed as means ±SD. Abbreviations: DAPI, 4′,6-diamidino-2-phenylindole; iPSC-CMs, induced pluripotent stem cell-derived cardiomyocytes; *LAMP-2*, lysosomal-associated membrane protein type 2; mROS, mitochondrial oxidative stress; NAC, *N*-acetylcysteine; ROS, reactive oxygen species; TUNEL, terminal deoxynucleotidyl transferase dUTP nick end labeling; WT, wild-type